Annals of R.S.C.B., ISSN:1583-6258, Vol. 25, Issue 6, 2021, Pages. 10552 - 10570
Received 25 April 2021; Accepted 08 May 2021.

Leishmanicidal Activity of Quinoline Derivatives: Synthesis, Evaluation and Computational Studies

Ravinder Sharma[1], Divya Yadav[1], Sapna Joshi[1] and Rakesh Yadav[2]*
[1]Department of Pharmacy, Banasthali Vidyapith, Banasthali-304022, Rajasthan, India
[2]Amity Institute of Pharmacy, Amity University, Manesar, Gurugram, Haryana
*rakesh_pu@yahoo.co.in

ABSTRACT

Newer 3, 6, and 8-aminoquinoline substituted compoundsi.e. (10a-f, 11a-f and 12a-f) were synthesized and evaluated for their in-vitro antileishmanial activity against promastigote form of *Leishmania donovani*. Among the tested analogues, seven compounds (10a, 10f, 11f, 12a, 12c, 12d and 12f) exhibited significant antileishmanial activity in comparison to standard drug sitamaquine. Docking study was also performed to understand the interaction of newly synthesized compounds with binding sites. Aminoquinolinessubstituted with phthalimide(10f, 2f and 3f) exhibited better binding affinity (-8.5, -8.2 and -8.4)in respect to standarddrug (-6.9). In silico ADME prediction studies depicted that the newly synthesized compounds obeyed Lipinski's rule of five, exhibited better absorption and toxicity profile as compared to the standard drug.

Keywords
Antileishmanial activity, Leishmania donovani, molecular docking, quinolines, ADME.

INTRODUCTION

Leishmaniasis is a potential chronic and neglected infectious disease caused by protozoan parasite of genus Leishmania [1]. The repercussions of this parasitic disease on public health have been underemphasized owing to lack of awareness, unhygienic and unhealthy living conditions specifically in tropical and subtropical regions [2-4].The prevalence of this parasitic disease is also related to an increase in Leishmania HIV co-infection in several parts of the world, including many European countries [5]. About 1.5 million people are affected by this disease annually, while another billion people live in endemic areas [6-7].So, the control of leishmaniasis remains a pressing problem with constantly surging cases worldwide, moreover the severity of the disease can be realized from the fact that this is ranked second only to malaria in chronic health epidemics.

Initially, leishmaniasis was classified based on its geographical distribution, antigenic properties, clinical manifestations, and vector types [8-11]. However, as technology advanced, it was discovered that pathological and geographical criteria were indeed insufficient, and techniques such as biochemical and molecular analysis and the polymorphism pattern depicted by kinetoplast DNA markers have been used instead [12-16]. There are about thirty recognized species of leishmania, with about twenty of them being pathogenic to humans.Recently Fraga and his fellow researchers analyzed and isolates strains from diverse geographical origins by utilizing sequences of the highly conserved 70-kDa heat shock protein [17].Few species of leishmania along with geographical distribution that are pathogenic to human are given in **(Table 1)**.

S.No.	Name of the organism	Geographical distribution
1.	*L. donovani*	Indian subcontinent, Sudan, Iran, Kenya, Saudi Arabia and China.
2.	*L. infantum*	Italy, Morocco, Portugal, Spain, Syria, Tunisia, France, Turkey, Greece Yemen, Brazil, Colombia, Ecuador, Mexico, Nicaragua, Paraguay, Suriname, and Venezuela
3.	*L. tropica*	Israel, Greece, Iran, Afghanistan, Azerbaijan, Iraq, Algeria, Tunisia, Turkey, and Yemen

Annals of R.S.C.B., ISSN:1583-6258, Vol. 25, Issue 6, 2021, Pages. 10552 - 10570
Received 25 April 2021; Accepted 08 May 2021.

4.	*L. aethiopica*	Ethiopia, Kenya
5.	*L. major*	Afghanistan, Algeria, Chad, Iran, Iraq, Israel, Libya, Mauritania, Morocco, Syria, and Sudan
6.	*L. mexicana*	Colombia, Costa Rica, Dominican Republic, Ecuador, Mexico, Panama, and Venezuela
7.	*L. amazonensis*	Bolivia, Brazil, Colombia, Costa Rica, Ecuador, French Guyana, Panama, Peru, and Venezuela
8.	*L. panamensis*	Belize, Colombia, Costa Rica, Ecuador, Honduras, Nicaragua, Panama, and Venezuela
9.	*L. braziliansis*	Argentina, Belize, Bolivia, Brazil, Colombia, Costa Rica, Ecuador, Guatemala, Honduras, and Nicaragua

Table (1): - Geographical distribution of various leishmania protozoans

There are no reliable vaccines against leishmania infection because of the adverse effects, so the treatment is primarily based on chemotherapy with pentavalent antimonial, amphotericin B, and pentamidine. Miltefosine is another medication used to treat leishmaniasis [18-20]. However, resistance to this medication is caused by a single point mutation in the leishmania. As a result, considerable effort has been required for detection and production of novel therapeutic agents.

Heterocycles are an imperative class of compounds that accounts for nearly half of all recognized medicinal compounds such as biomolecules, vitamins and biologically active compounds [21-24].Amid all heterocycles, the quinoline derivatives exhibits wide variety of biological activities in various areas such as hematology, virology, CNS, stomach cancer and brain tumors and other proliferative diseases [25-27].The present paper describes synthesis of 3,6 and 8 amino substituted quinoline derivatives with their leishmanicidal profile against*L.donovani*. Docking and ADME profile of the newly synthesized derivatives has also been reported.

MATERIALS AND METHODS

All chemicals used were of commercially available reagent grade and were used without further purification. Melting points were determined on Veego melting point apparatus and were uncorrected. Proton (^{1}H) nuclear magnetic resonance spectroscopy was performed using a Brucker AC-400F, 400 MHz spectrophotometer for solutions in deuteriochloroform and deuterated dimethylsulfoxide and are reported in parts per million (ppm) downfield from tetramethylsilane (Me Si) as internal reference. The spin multiplicities are indicated by the symbols, s (singlet), d (doublet), t (triplet), q (quartet), and m (multiplet). Reaction's progress was monitored by precoated (20x20 cm Silica gel 60 F254) plates which were procured from E. Merck, Germany. Spots were visualized using UV-chamber (Perfit India). Anhydrous sodium sulphate was utilized as drying agent.

General procedure for the synthesis

The synthesis of various quinoline derivatives was performed by refluxing equimolar concentration of 4-hydroxy benzoic acid**(1)** and 1, 2-dichloroethane**(2)** under stirring in the presence of ethyl methyl ketone and potassium carbonate at 80ºC for two hours. Excess solvent was removed under vacuum to get an intermediate product4-(2-chloroethoxy)benzoic acid**(3)**which in the presence of 1-ethyl-3-(3-dimethylaminopropyl)-carbodiimide (EDCI) was treatedwithvarious aminoquinolines(**4-6**) to produce the benzamide derivatives (**7-9**). Thesebenzamide intermediates (**7-9**)were further reacted with respective amine such as piperidine, dimethyl amine, morpholine, pyrrolidine, diethyl amine and phthalimide to give desired quinoline derivatives (10a-f, 11a-f and 12a-f) as per (**Scheme 1)**.

Annals of R.S.C.B., ISSN:1583-6258, Vol. 25, Issue 6, 2021, Pages. 10552 - 10570
Received 25 April 2021; Accepted 08 May 2021.

Scheme 1

Annals of R.S.C.B., ISSN:1583-6258, Vol. 25, Issue 6, 2021, Pages. 10552 - 10570
Received 25 April 2021; Accepted 08 May 2021.

BIOLOGICAL EVALUATION

For preparing the stock solutions i.e. (10 mg/mL) of the synthetic quinoline derivatives about 10mg of the sample compounds was dissolved in 1ml of DMSO. Further to get required dilutions varying from 2.5 µg/mL to 100 µg/mL each stock solution was further diluted with Roswell Park Memorial Institute (RPMI) complete media.The influence of tested molecules upon the survivability of promastigote form of *Leishmania donovani* has been estimated by measuring the metabolism of MTT [3-(4,5-dimethylthiazol-2-yl)-2,5-diphenyl-tetrazolium bromide] following incubation period of 96-h. Cells were inoculated at 1×10^6 /100 µL RPMI-1640 in each cavity of 96-well flat bottom microtiter plates. Further to accomplish preferred concentrations, 100 µL of media per well with different concentrations of synthesized compounds (2.5 µg/ml to 100 µg/ml) or standard drug (2.5 µg/ml to 50 µg/ml) dissolved in DMSO was added in triplicate [28].The plates were incubated at 37 °C for a period of 72 h before addition of MTT (10 µL per well of a 5 mg mL^{-1} PBS stock) and then plates were incubated further for 4–5 hours in CO_2 incubator. MTT processing was stopped and formazan crystals solubilized by adding 50 µL of DMSO per well and incubated overnight at 37 °C . The relative amount of formazan per well produced by viable cells was measured photometrically at 590 nm. The experiments were performed in triplicate for the determination of sensitivity of each compound.

COMPUTATIONAL STUDIES

Molecular Docking

The molecular docking procedure was used to predict the binding interactions between the quinoline derivatives and the binding pocket of the enzyme adenine phosphoribosyltransferase from *Leishmania donovani for* further pharmacological evaluation.

Preparation of target for docking analysis

The 3D crystal structure of the adenine phosphoribosyltransferase from *Leishmania donovani* (PDB ID: 1QCD with a resolution of 2.48˚A) was retrieved from the protein databank.After retrieving the structure all the water and ions molecules were relinquished and the hydrogen atoms were added to the protein by the protonation using the DS visualizer (version v20.1.0.19295) software [29].The active site was determined using site sphere method of Discovery visualizer. Energy minimization of protein was performed with DS using CHARMm(Chemistry at Harvard Macromolecular Mechanics) and MMFF94 (Merck molecular) force field.

3D Structure Validation

To check the compatibility of atomic models (3D) with its own primary amino acid sequences (1D), The VERIFY3D server was used [30-31]. The Verify 3D evaluated that the predicted protein has 86.44%% residues with an average 3D-1D score ≥0.2 which signify the consistency and reliability of the 3D model because the ideal score values for Verify-3D should be 80% as shown in **(Figure 1)**.

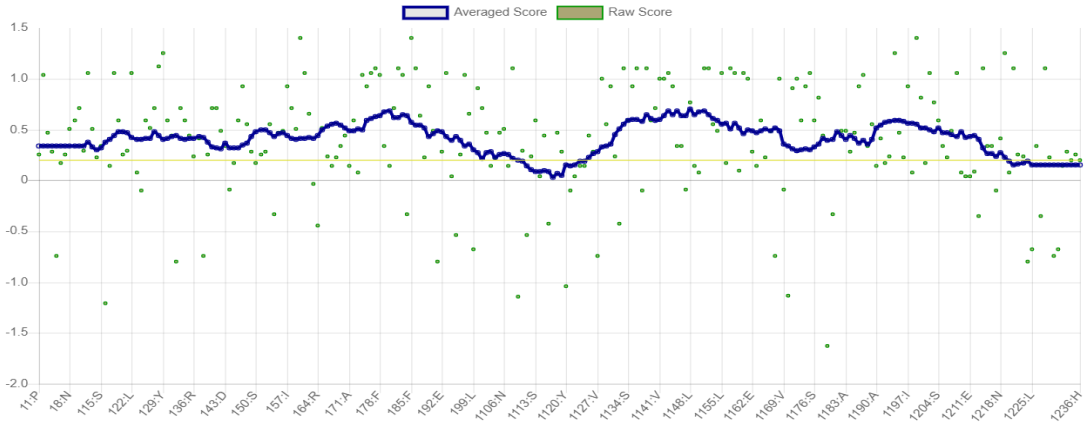

Figure (1):-Stereochemical analysis of 1QCD showing 86.44% of the residues have averaged 3D-1D score >= 0.2

Annals of R.S.C.B., ISSN:1583-6258, Vol. 25, Issue 6, 2021, Pages. 10552 - 10570
Received 25 April 2021; Accepted 08 May 2021.

Preparation of ligand for docking analysis

Each ligand structure was built by Chem3D pro version 12.0.2.1076 and optimized using mmff94 force field and employing conjugate gradients optimization algorithm with around 200 number of steps in pyrx software. After energy minimisation ligands are converted into pdbqt format using OpenBableGUI software embedded in pyrx [32].

Docking methodology and analysis

Computational Docking is performed to get various probable conformations and orientations of the ligands with binding site. The grid centre for docking was set X= 28.9567, Y= 28.6635 and Z= 7.588 for 1QCD, after this virtual screening was carried by rigid molecular docking into the active site of protein. Throughout the virtual screening, the ligand molecules were flexible and macromolecule was kept as rigid. Finally, the result of binding energy was extracted from the software.

Drug-likeness and ADMET evaluation

Inadequate pharmacokinetic and toxicity studies lead to failure of drug development process in the final stages. Therefore, in order to escalate drug discovery process, primary assessment of pharmacokinetic and toxicity studies is the mandate step [33-35].

Drug-likeness

Drug-likeness is an important aspect in drug development for screening of drug molecules promptly. This parameter is being used as a process to corelate physicochemical aspect of a drug molecule with its biopharmaceutical aspect in human body, particularly its impact on bioavailability in oral route [36].Therefore, all the synthetic derivatives were assessed for their druglike nature under Lipinski's rules of five by employing DruLiTo software [37].As per Lipinski's rule, the Log P of "drug-like" molecules should be less than 5, molecular weight (M.W.) below 500, Total polar surface area under 140 and number of hydrogen bond acceptors (HBA) as well as number of hydrogen bond donors (HBD) below 10 and 5 respectively [38].

ADMET analysis

For assessment of different pharmacokinetic properties like absorption, distribution, metabolism, excretion, and toxicity of synthetic compounds within the human body ADMETlab web platform was used [39]. The ADMETlab envisaged the Human Intestinal Absorption (HIA+ or HIA-), Blood-Brain Barrier Penetration (BBB+ or BBB-), Caco-2 Permeability (permeable or non-permeable), Human Hepatotoxicity (H-HT), Solubility i.e., LogS value and Acute toxicity (LD_{50}).

RESULTS&DISCUSSION

Spectral Data

4-(2-(Piperidin-1-yl)-ethoxy)-*N*-(quinolin-3-yl)-benzamide (10a)

Yield: 66%, m.p: 223-226°C**FT-IR (KBr, cm^{-1}):**1109 (C-O), 1322 (C-N), 1492 (C=C), 1657 (C=O), 3253 (-NH-).**^{1}H-NMR** (DMSO-d_6): δ 1.71 (m, 6H, $(-CH_2)_3$, piperidine), 2.50 (t, 4H, $(-NCH_2)_2$ piperidine), 2.88 (t, 2H, $-CH_2-$), 4.26 (t, 2H, $-CH_2-$), 6.06 (s, 1H, -NH), 6.90 (dd, 2H, CH, Ar), 7.11 (dd, 2H, CH, Ar), 7.62 (m, 3H, -CH, quinoline) 8.0 (d, 2H, CH, quinoline), and 8.57 (s, 1H, CH, quinoline) ppm. **Elemental analysis** ($C_{23}H_{25}N_3O_2$); **Calcd**. C, 73.57; H, 6.71; N, 11.19; O, 8.52; **found**: C, 73.42; H, 6.38; N, 11.01.

4-(2-(Dimethylamino)ethoxy)-*N*-(quinolin-3-yl)benzamide (10b)

Yield: 68%, m.p: 196-198°C, **FT-IR (KBr, cm^{-1}):** 1060 (C-O), 1318 (C-N), 1641 (C=O), 3062 (C=C-H), 3353 (-NH-).**^{1}H-NMR** (DMSO-d_6): δ 2.29 (s, 6H, $(-N(CH_3)_2)$, 2.76 (t, 2H, $-CH_2-$), 4.23 (t, 2H, $-CH_{2-}$),6.09 (s, 1H, -NH), 6.87 (dd, 2H, CH, Ar), 6.53 (dd, 2H, CH, Ar), 7.69 (m, 3H, -CH, quinoline) 8.0 (d, 2H, CH, quinoline), and 8.53 (s, 1H, CH, quinoline) ppm. **Elemental analysis** ($C_{20}H_{21}N_3O_2$); **Calcd**. C, 71.62; H, 6.31; N, 12.53; O, 9.54 **found**: C, 71.40; H, 6.00; N, 12.32.

4-(2-(Morpholino)ethoxy)-*N*-(quinolin-3-yl)benzamide (10c)

Yield: 65%, m.p: 239-242°C, **FT-IR (KBr, cm^{-1}):**1113 (C-N), 1459 (C-H), 1324 (C=N), 1457 (C=C), 1631 (C=O), 3293 (-NH-). **^{1}H-NMR** ($CDCl_3$): δ 2.45 (t, 4H, $(-NCH_2)_2$), 2.89 (t, 2H, $-CH_2-$), 4.28 (t, 2H, $-CH_2-$), 3.59 (t, 4H, $(-OCH_2)_2$), 4.28 (t,

Annals of R.S.C.B., ISSN:1583-6258, Vol. 25, Issue 6, 2021, Pages. 10552 - 10570
Received 25 April 2021; Accepted 08 May 2021.

2H, -CH_2-), 5.98 (s, 1H, -NH), 7.10 (dd, 2H, CH, Ar), 8.05 (dd, 2H, CH, Ar), 7.69 (m, 3H, -CH, quinoline) 8.04 (d, 2H, CH, quinoline), and 8.38 (s, 1H, CH, quinoline) ppm. **Elemental analysis** ($C_{22}H_{23}N_3O_3$); **Calcd**. C, 70.01; H, 6.14; N, 11.13; O, 12.72; **found**: C, 69.79; H, 5.84; N, 12.51.

4-(2-(Pyrrolidin-1-yl)ethoxy)-*N*-(quinolin-3-yl)benzamide (10d)

Yield: 62%, m.p: 229-232°C, **FT-IR (KBr, cm^{-1}):**1078 (C-0), 1323 (C=N), 1446 (C=C), 1635 (C=O), 3365 (-NH-).**^{1}H-NMR** (DMSO-d_6): δ 1.87 (t, 4H, (-CH_2-)$_2$, pyrrolidine), 2.86 (t, 2H, -CH_2-), 2.98 (t, 4H, (-NCH_2)$_2$ pyrrolidine), 4.25 (t, 2H, -CH_2-), 6.23 (s, 1H, -NH), 7.10 (d, 2H, CH, Ar), 8.03 (d, 2H, CH, Ar), 7.62 (m, 3H, -CH, quinoline) 8.04 (d, 2H, CH, quinoline), and 8.38 (s, 1H, CH, quinoline) ppm. **Elemental analysis** (($C_{22}H_{23}N_3O_2$); **Calcd**. C, 73.11; H, 6.41; N, 11.63; O, 8.85; **found**: C, 72.89; H, 6.10; N, 11.44.

4-(2-(Diethylamino)ethoxy)-*N*-(quinolin-3-yl)benzamide (10e)

Yield: 56%, m.p: 216-219°C, **FT-IR (KBr, cm^{-1}):**1010 (C-O), 1282 (C-N),1665 (C=O), 3048 (C=C-H), 3231 (-NH-).**^{1}H-NMR** (DMSO-d_6): δ 0.96 (t, 6H, (-CH_3)$_2$), 2.64 (q 4H, -N-(-CH_2)$_2$), 2.85 (t, 2H, -CH_2), 4.26 (t, 2H, -CH_2-), 6.70 (s, 1H, -NH), 7.12 (dd, 2H, CH, Ar), 8.02 (dd, 2H, CH, Ar), 7.52 (m, 3H, -CH, quinoline) 8.00 (d, 2H, CH, quinoline), and 8.61 (s, 1H, CH, quinoline) ppm. **Elemental analysis** ($C_{22}H_{25}N_3O_2$); **Calcd**. C, 72.70; H, 6.93; N, 11.56; O, 8.80; **found**: C, 72.45; H, 6.59; N, 11.37.

4-(2-(1,3-Dioxoisoindolin-2-yl)ethoxy)-*N*-(quinolin-3-yl)benzamide (10f)

Yield: 54, m.p: 312-315°C, **FT-IR (KBr, cm^{-1}):** 1025 (C-O), 1447 (C=C), 1645 (C=O), 3004 (C-H), 3262 (-NH-). **^{1}H-NMR** ($CDCl_3$): δ 2.98 (t, 2H, -CH_2-), 4.32 (t, 1H, -CH_2-), 6.30 (s, 1H, -NH), 7.21 (d, 2H, CH, Ar), 7.99 (d, 2H, -CH, Ar), 7.87 (m, 4H, CH, phthalimide), 7.50 (m, 3H, -CH, quinoline) 8.07 (d, 2H, CH, quinoline), and 8.67 (s, 1H, CH, quinoline) ppm. **Elemental analysis** ($C_{26}H_{19}N_3O_4$); **Calcd**. C, 71.39; H, 4.38; N, 9.61; O, 14.63; **found**: C, 71.15; H, 4.16; N, 9.45.

4-(2-(Piperidin-1-yl)ethoxy)-*N*-(quinolin-6-yl)benzamide (11a)

Yield: 62%, m.p: 262-265°C **FT-IR (KBr, cm^{-1}):** 1106 (C-O), 1323 (C-N), 1473 (C=C), 1648 (C=O), 3248 (-NH-).**^{1}H-NMR** (DMSO-d_6): δ 1.46 (m, 6H, (-CH_2)$_3$, piperidine), 2.43 (t, 4H, (-NCH_2)$_2$, piperidine), 2.64 (t, 2H, -CH_2-), 4.36 (t, 2H, -CH_2-), 6.49 (s, 1H, -NH), 6.79 (dd, 2H, CH, Ar), 7.86 (dd, 2H, CH, Ar), 7.23 (m, 2H, CH, quinoline), 7.43 (t, 1H, CH, quinoline), 7.47 (d, 1H, -CH, quinoline), 7.80 (d, 1H, CH, quinoline), and 8.85 (d, 1H, CH, quinoline) ppm. **Elemental analysis** ($C_{23}H_{25}N_3O_2$); **Calcd**. C, 73.57; H, 6.71; N, 11.19; O, 8.52; **found**: C, 73.42; H, 6.30; N, 11.14.

4-(2-(Dimethylamino)ethoxy)-*N*-(quinolin-6-yl)benzamide (11b)

Yield: 68%, m.p: 213-216°C, **FT-IR (KBr, cm^{-1}):** 1019 (C-O), 1112 (C-N), 1455 (C=C), 1646 (C=O), 3239 (-NH-).**^{1}H-NMR** (DMSO-d_6): δ 2.16 (s, 6H, (-N(-CH_3)$_2$), 2.72 (t, 2H, -CH_2-), 4.29 (t, 2H, -CH_2-), 6.39 (s, 1H, -NH), 6.79 (dd, 2H, CH, Ar), 7.86 (dd, 2H, CH, Ar), 7.23 (t, 1H, CH, quinoline), 7.37 (m, 2H, CH, quinoline), 7.45 (d, 1H, -CH, quinoline), 7.97 (d, 1H, CH, quinoline), and 8.57 (d, 1H, CH, quinoline) ppm. **Elemental analysis** ($C_{20}H_{21}N_3O_2$); **Calcd**. C, 71.62; H, 6.31; N, 12.53; O, 9.54; **found**: C, 71.47; H, 5.92; N, 12.47.

4-(2-(Morpholino)ethoxy)-*N*-(quinolin-6-yl)benzamide (11c)

Yield: 72%, m.p: 274-277°C, **FT-IR (KBr, cm^{-1}):** 1116 (C-O), 1204 (C-N), 1454 (C=C), 1665 (C=O), 3279 (-NH-)**^{1}H-NMR** ($CDCl_3$): δ 2.50 (t, 4H, (-NCH_2)$_2$,morpholine), 2.69 (t, 2H, -CH_2-), 4.06 (t, 2H, -CH_2-), 3.57 (t, 4H, (-OCH_2)$_2$, morpholine), 6.68 (s, 1H, -NH), 6.71 (dd, 2H, CH, Ar), 7.2 (dd, 2H, CH, Ar), 7.32 (t, 1H, CH, quinoline), 7.42 (m, 2H, CH, quinoline), 7.48 (d, 1H, -CH, quinoline), 7.63 (d, 1H, CH, quinoline), and 8.47 (d, 1H, CH, quinoline) ppm. **Elemental analysis** ($C_{22}H_{23}N_3O_3$); **Calcd**. C, 70.01; H, 6.14; N, 11.13; O, 12.72; **found**: C, 69.86; H, 5.76; N, 11.08

4-(2-(Pyrrolidin-1-yl)ethoxy)-*N*-(quinolin-6-yl)benzamide (11d)

Yield: 67%, m.p: 251-254°C, **FT-IR (KBr, cm^{-1}):** 1018 (C-O), 1328 (C-N), 1473 (C=C), 1636 (C=O), 3297 (-NH-).**^{1}H-NMR** (DMSO-d_6): δ 1.65 (t, 4H, (-CH_2-)$_2$, pyrrolidine), 2.66 (t, 2H, -CH_2-), 2.88 (t, 4H, (-NCH_2)$_2$ pyrrolidine), 4.32 (t, 2H, -CH_2-), 6.43 (s, 1H, -NH), 6.79 (dd, 2H, CH, Ar), 7.45 (dd, 2H, CH, Ar), 7.38 (t, 1H, CH, quinoline), 7.22 (m, 2H, CH, quinoline), 7.46 (d, 1H, -CH, quinoline), 7.76 (d, 1H, CH, quinoline), and 8.67 (d, 1H, CH, quinoline) ppm. **Elemental analysis** ($C_{22}H_{23}N_3O_2$); **Calcd**. C, 73.11; H, 6.41; N, 11.63; O, 8.85; **found**: C, 72.95; H, 6.01; N, 11.58.

Annals of R.S.C.B., ISSN:1583-6258, Vol. 25, Issue 6, 2021, Pages. 10552 - 10570
Received 25 April 2021; Accepted 08 May 2021.

4-(2-(Diethylamino)ethoxy)-*N*-(quinolin-6-yl)benzamide (11e)

Yield: 61%, m.p: 232-235°C, **FT-IR (KBr, cm^{-1}):** 1024 (C-O), 1245 (C-N),1656 (C=O), 3058 (C=C-H), 3341 (-NH-).**^{1}H-NMR** (DMSO-d_6): δ 0.93 (t, 6H, $(-CH_3)_2$), 2.37 (q, 4H, $-N-(CH_2)_2$), 2.95 (t, 2H, $-CH_2$), 4.39 (t, 2H, $-CH_2$-), 6.48 (s, 1H, -NH), 7.08 (dd, 2H, CH, Ar), 8.06 (dd, 2H, CH, Ar), 7.34 (t, 1H, CH, quinoline)7.52 (m, 2H, -CH, quinoline), 7.60 (d, 1H, -CH, quinolin) 8.00 (d, 1H, CH, quinoline), and 8.76 (d, 1H, CH, quinoline) ppm. **Elemental analysis** ($C_{22}H_{25}N_3O_2$); **Calcd**. C, 72.70; H, 6.93; N, 11.56; O, 8.80; **found**: C, 72.55; H, 6.50; N, 11.51.

4-(2-(1,3-Dioxoisoindolin-2-yl)ethoxy)-*N*-(quinolin-6-yl)benzamide (11f)

Yield: 54%, m.p: 334-337°C, **FT-IR (KBr, cm^{-1}):** 1053(C-O), 1448 (C=C), 1556 (N-H), 1606 (C=C),1653 (C=O), 3281 (-NH-). **^{1}H-NMR** ($CDCl_3$): δ 3.98 (t, 2H, $-CH_2$-), 4.43 (t, 1H, $-CH_2$-), 6.10 (s, 1H, -NH), 7.05 (d, 2H, CH, Ar), 7.95 (d, 2H, -CH, Ar), 7.81 (m, 4H, CH, phthalimide), 7.08 (dd, 2H, CH, Ar), 8.06 (dd, 2H, CH, Ar), 7.47 (t, 1H, CH, quinoline)7.67 (m, 2H, -CH, quinoline), 7.72 (d, 1H, -CH, quinoline) 8.06 (d, 1H, CH, quinoline), and 8.78 (d, 1H, CH, quinoline) ppm. **Elemental analysis** ($C_{26}H_{19}N_3O_4$); **Calcd**. C, 71.39; H, 4.38; N, 9.61; O, 14.63; **found**: C, 71.25; H, 4.11; N, 9.57.

4-(2-(Piperidin-1-yl)ethoxy)-*N*-(quinolin-8-yl)benzamide (12a)

Yield: 69%, m.p: 216-219°C **FT-IR (KBr, cm^{-1}):** 1072 (C-O), 1328 (C-N), 1488 (C=C), 1648 (C=O), 3370 (-NH-).**^{1}H-NMR** (DMSO-d_6): δ 0.89 (m, 6H, $(-CH_2)_3$, piperidine), 1.91 (t, 4H, $(-NCH_2)_2$ piperidine), 2.62 (t, 2H, $-CH_2$-), 4.00 (t, 2H, $-CH_2$-), 6.32 (s, 1H, -NH), 7.01 (dd, 2H, CH, Ar), 7.41 (dd, 2H, CH, Ar), 7.78 (m, 4H, -CH, quinoline) 8.0 (d, 1H, CH, quinoline), and 8.47 (d, 1H, CH, quinoline) ppm. **Elemental analysis** ($C_{23}H_{25}N_3O_2$); **Calcd**. C, 73.57; H, 6.71; N, 11.19; O, 8.52; found: C, 73.25; H, 6.36; N, 10.92.

4-(2-(Dimethylamino)ethoxy)-*N*-(quinolin-8-yl)benzamide (12b)

Yield: 73%, m.p: 191-193°C, **FT-IR (KBr, cm^{-1}):** 1013 (C-O), 1309 (C-N), 1442 (C=C), 1671 (C=O), 3367 (N-H).**^{1}H-NMR** (DMSO-d_6): δ 1.39 (s, 6H, $(-N(CH_3)_2)$, 2.16 (t, 2H, $-CH_2$-), 3.23 (t, 2H, $-CH_2$-), 6.50 (s, 1H, -NH), 6.90 (dd, 2H, CH, Ar), 7.31 (dd, 2H, CH, Ar), 7.57 (m, 4H, -CH, quinoline) 7.98 (d, 1H, CH, quinoline), and 8.39 (d, 1H, CH, quinoline) ppm. **Elemental analysis** ($C_{20}H_{21}N_3O_2$); **Calcd**. C, 71.62; H, 6.31; N, 12.53; O, 9.54; **found**: C, 71.33; H, 5.98; N, 12.22.

4-(2-(Morpholino)ethoxy)-*N*-(quinolin-8-yl)benzamide (12c)

Yield: 74%, m.p: 223-227°C, **FT-IR (KBr, cm^{-1}):** 1109 (C-O), 1322 (C-N), 1481 (C=C), 1656 (C=O), 3371 (-NH-). **^{1}H-NMR** ($CDCl_3$): δ 2.50 (t, 4H, $(-NCH_2)_2$, morpholine), 2.59 (t, 2H, $-CH_2$-), 3.45 (t, 2H, $-CH_2$-), 3.50 (t, 4H, $(-OCH_2)_2$, morpholine), 6.10 (s, 1H, -NH), 6.76 (dd, 2H, CH, Ar), 7.28 (dd, 2H, CH, Ar), 7.67 (m, 4H, -CH, quinoline) 7.78 (d, 1H, CH, quinoline), and 8.30 (d, 1H, CH, quinoline) ppm. **Elemental analysis** ($C_{22}H_{23}N_3O_3$); **Calcd**. C, 70.01; H, 6.14; N, 11.13; O, 12.72; **found**: C, 69.79; H, 5.82; N, 10.86.

4-(2-(Pyrrolidin-1-yl)ethoxy)-*N*-(quinolin-8-yl)benzamide (12d)

Yield: 67%, m.p: 223-227°C, **FT-IR (KBr, cm^{-1}):** 1011 (C-O), 1322 (C-N), 1484 (C=C), 1671 (C=O), 3346 (-NH-).**^{1}H-NMR** (DMSO-d_6): δ 1.15 (t, 4H, $(-CH_2-)_2$, pyrrolidine), 1.97 (t, 4H, $(-NCH_2)_2$ pyrrolidine),2.26 (t, 2H, $-CH_2$-), 3.37 (t, 2H, $-CH_2$-), 6.55 (s, 1H, -NH), 6.86 (dd, 2H, CH, Ar), 7.32 (dd, 2H, CH, Ar), 7.62 (m, 4H, -CH, quinoline) 7.78 (d, 1H, CH, quinoline), and 8.39 (d, 1H, CH, quinoline) ppm. **Elemental analysis** ($C_{22}H_{23}N_3O_2$); **Calcd**. C, 73.11; H, 6.41; N, 11.63; O, 8.85; **found**: C, 72.81; H, 6.07; N, 11.35.

4-(2-(Diethylamino)ethoxy)-*N*-(quinolin-8-yl)benzamide (12e)

Yield: 63%, m.p: 210-213°C, **FT-IR (KBr, cm^{-1}):** 1078 (C-O), 1230 (C-N), 1456 (C=C), 1662(C=O), 3398 (N-H).**^{1}H-NMR** (DMSO-d_6): δ 0.91 (t, 6H, $(-CH_3)_2$), 1.64 (q, 4H, $-N-(CH_2)_2$), 2.05 (t, 2H, $-CH_2$), 3.06 (t, 2H, $-CH_2$-), 6.70 (s, 1H, -NH), 6.96 (dd, 2H, CH, Ar), 7.54 (dd, 2H, CH, Ar), 7.71 (m, 4H, -CH, quinoline) 7.88 (d, 1H, CH, quinoline), and 8.43 (d, 1H, CH, quinoline) ppm. **Elemental analysis** ($C_{22}H_{25}N_3O_2$); **Calcd**. C, 72.70; H, 6.93; N, 11.56; O, 8.80; **found**: C, 72.40; H, 6.56; N, 11.28.

4-(2-(1,3-Dioxoisoindolin-2-yl)ethoxy)-*N*-(quinolin-8-yl)benzamide (12f)

Yield: 54%, m.p: 303-306°C, **FT-IR (KBr, cm^{-1}):** 1189 (C-O), 1441 (C=C), 1661 (C=O), 3104(C=C-H), 3309 (-NH-). **^{1}H-NMR** ($CDCl_3$): 3.38 (t, 2H, $-CH_2$-), 4.39 (t, 1H, $-CH_2$-), 6.33 (s, 1H, -NH), 7.11 (d, 2H, CH, Ar), 7.89 (d, 2H, -CH, Ar),

Annals of R.S.C.B., ISSN:1583-6258, Vol. 25, Issue 6, 2021, Pages. 10552 - 10570
Received 25 April 2021; Accepted 08 May 2021.

7.83 (m, 4H, CH, phthalimide), 7.60 (m, 4H, -CH, quinoline) 8.11 (d, 1H, CH, quinoline), and 8.82 (s, 1H, CH, quinoline) ppm. **Elemental analysis** ($C_{26}H_{19}N_3O_4$); **Calcd**. C, 71.39; H, 4.38; N, 9.61; O, 14.63; **found**: C, 71.19; H, 4.15; N, 9.37.

The molecular structures of these synthetic quinoline derivatives were established on the basis of their spectral data. The infrared spectra of various synthesized compounds showed an absorption band at 3239-3398 cm-1 characteristics of NH, strong peak around 1631-1665 conforming C=O amide linkage and bands around 1441–1492 cm-1 and 1010-1198 cm-1 corresponding to C=C asymmetric aromatic stretching and C–O respectively were also observed.

For 1H NMR, spectra of the synthesized compounds were found to be in constancy with the proposed structures. Moreover, the number of the integrated protons in the spectra correspond to the probable number of aromatic protons in each case. The spectra of various compounds revealed the signals of aromaticity, substituted dimethyl and diethyl and methylene of aliphatic chain. The singlet at δ 6.00-6.68 ppm revealed the presence of NH group. The triplet at around δ 2.00-2.98 ppm and a triplet at around δ 3.06-4.38 ppm accounted for two methylene group of aliphatic chain. The various aromatic protons appear as complex system in the range between δ 6.70-8.85 ppm.

Biological Activity

As a prefatory evaluation, the leishmanicidal effect of the synthetic quinolines derivative was evaluated on promastigote form of *L. donovani* which is the causative agent of most severe form of leishmaniasis (visceral leishmania especially in Sudan and other developing countries) and the inhibitory concentration that reduces the parasitic growth by 50% (IC_{50}) as listed in **(Table 2)** was calculated by projecting percentage inhibition against concentration of drug using statistical analysis.

S.No.	**Compound No.**	**IC_{50} (μg/mL)**
1.	**10a**	8.60
2.	**10b**	14.70
3.	**10c**	10.02
4..	**10d**	10.97
5.	**10e**	14.50
6.	**10f**	6.22
7.	**11a**	11.60
8.	**11b**	22.96
9.	**11c**	10.89
10.	**11d**	14.00
11.	**11e**	18.66
12.	**11f**	7.08
13.	**12a**	8.34
14.	**12b**	15.97
15.	**12c**	9.83
16.	**12d**	9.26
17.	**12e**	15.64
18.	**12f**	6.05
19.	**Sitamaquine**	10.09

Table (2):-IC_{50} of the various compounds and positive control*

Most of the derivatives demonstrated antileishmanial activity against *L. donovani* with IC_{50} value ranging from 6.05 to 22.96 µg/ml and among these compound 3f is most potent with IC_{50} value of 6.05 followed by other derivatives such as 10f, 11f,12a, 10a, 12d and 12c with IC_{50} values of 6.22, 7.08, 8.34, 8.60, 9.26 and 9.83 respectively. Some derivatives such as 11c, 10c, 10d and 11a displayed comparable activity to standard drug sitamaquine.

Annals of R.S.C.B., ISSN:1583-6258, Vol. 25, Issue 6, 2021, Pages. 10552 - 10570
Received 25 April 2021; Accepted 08 May 2021.

Molecular Docking

Binding energy (kcalmol^{-1}) is the significant key parameter which is generated as an outcome of molecular docking. It gives the indication of affinity and intensity of the interaction among the ligand and the receptor. The binding energy and intensity of interaction are reciprocal to each other i.e., the more is the binding energy, the less will be intensity of the interaction and vice versa. Therefore, during docking studies the ligand which displays the minimal binding energy is considered as ideally suited for further evaluation.So, all the docked conformations were analysed and the best-scored pose for each compound was selected for further interaction studies. The docking scores of various compounds are given in the **(Table 3)**.

S.No.	Compound Name	Docking Score (kcalmol^{-1})	Interacting Residues
1.	**10a**	**-7.9**	Lys186, Ser157, Leu156, Met129, Glu127, Pro126
2.	**10b**	**-7.1**	Ser157, Leu156, Met129, Glu127, Pro126, Phe79
3.	**10c**	**-7.5**	Lys186, Ser157, Leu156, Ala155, Met129, Glu127, Glu120, Tyr117
4.	**10d**	**-7.5**	Lys186, Ser157, Leu156, Ala155, Met129, Glu127, Pro126, Phe79
5.	**10e**	**-7.1**	Ile187, Lys186, Ser157, Leu156, Ala155, Met129, Glu127, Pro126
6.	**10f**	**-8.5**	Lys186, Ala183, Ser157, Leu156, Ala155, Met129, Glu127, Pro126
7.	**11a**	**-7.4**	Lys186, Ala183, Ser157, Leu156, Glu127, Pro126
8.	**11b**	**-6.4**	Ser157, Leu156, Glu127, Pro126, Ala124, Glu120
9.	**11c**	**-7.7**	Ser157, Leu156, Ala155, Glu127, Pro126, Glu120, Glu118
10.	**11d**	**-6.9**	Leu181, Leu156, Pro126, Ala124, Tyr117
11.	**11e**	**-6.6**	Ser157, Leu156, Glu127, Pro126
12.	**11f**	**-8.2**	Ala183, Ser157, Leu156, Ala155, Pro126, Ala124, Glu120, Pro116
13.	**12a**	**-7.9**	Lys186, Ala183, Leu156, Ala155, Pro126, Glu120
14.	**12b**	**-6.9**	Lys186, Ala183, Leu156, Pro126
15.	**12c**	**-7.8**	Ala183, Ser157, Leu156, Ala155, Pro126, Glu120, Tyr117
16.	**12d**	**-7.7**	Lys186,Ala183, Leu156, Met129, Pro126, Phe79
17.	**12e**	**-6.9**	Lys186, Ala183, Leu156, Pro126, Phe79
18.	**12f**	**-8.4**	Ile187, Ala183, Ser157, Leu156, Ala155, Pro126, Pro116
19.	**Sitamaquine**	**-6.9**	Ser157, Leu156, Pro126, Tyr117, Pro116

Table (3):-Comparison of docking energies (kcal/mol) of sitamaquine and quinoline derivatives.

The outcome of the docking results showed that all the compounds were well acclimatized in the active site of Leishmania enzyme. Among the various quinolone derivatives, the compound 1f was found to be the most active with a docking score of -8.5 followed by other compounds such as 3f and 2f with docking score of -8.4 and -8.2 respectively.

The docking conformation of the most active compound i.e.,**10f** exhibit conventional hydrogen bonding, pi-sigma interactions, pi-alkyl and pi-anion bonding with the active residues. Ala155, Leu156 and Ser157 shows conventional hydrogen bonding with one of the doubly bonded oxygen of the ligand and among these three Leu156 also exhibit pi-sigma interactions with one of the cyclic rings of quinoline. The nitrogen containing ring of the quinoline moiety also demonstrate alkyl linkage with Met129 where its cyclic ring exhibit pi-anion interactions with Glu127. The six membered rings of phthalimide display pi-alkyl linkage with Ala183 and Lys186 whereas five membered heterocyclic ring show alkyl linkage with Lys183. Pro126 also form pi-alkyl linkage with the six membered cyclic rings.

The docking pose of **11f** manifest hydrogen bonding, Vander waal, alkyl/pi-alkyl and pi-anion interactions of various amino acid residues of the active site. Ala155, Leu156 and Ser157 exhibit conventional hydrogen bonding interaction with doubly bonded oxygen atom of phthalimide and despite this Ala155 also display hydrogen interaction with the oxygen of hydroxybenzoic acid. Pro116, Pro126, Leu156 and Ala183 amino acid residues exhibit pi alkyl and alkyl

Annals of R.S.C.B., ISSN:1583-6258, Vol. 25, Issue 6, 2021, Pages. 10552 - 10570
Received 25 April 2021; Accepted 08 May 2021.

interactions with the drug molecule. Among these Pro126 exhibit alkyl interactions with both the rings of phthalimide moiety and nitrogen containing ring of quinoline, whereas Leu156 display interaction with both the rings of phthalimide as well as cyclic ring of hydroxy benzoic acid. The Pro116 and Ala183 show pi-alkyl linkage with six membered rings of phthalimide and hydroxy benzoic acid respectively. One of the cyclic rings of quinoline moiety also exhibit pi-anion interactions with Glu127.

Docking pose of second most active compound among two series i.e., **12f** with binding affinity of -8.4 kcal/mol exhibit conventional hydrogen bonding with Ala155 and Ser157. These two amino acid residues form hydrogen bonding with doubly bonded oxygen of phthalimide ring and Ala155 also exhibit hydrogen bonding with oxygen of hydroxy benzoic acid. Pro116, Pro126 and Leu156 display pi-alkyl interactions with the phthalimide moiety as well as with the nitrogen containing ring of quinoline. Amino acid residues such as Ala155, Ala183 and Ile187 manifest pi-alkyl linkage with hydroxy benzoic acid residue, Ala183 also exhibit Vander waal interactions with the doubly bonded oxygen of hydroxy benzoic acid.

The docking conformation of standard drug sitamaquine exhibit conventional hydrogen bonding as well as alkyl/pi-alkyl interactions with the various active residues of target molecule. The nitrogen of substituted secondary amine moiety of sitamaquine exhibit hydrogen bonding with the Tyr117, where other residue Ser157 showed hydrogen bonding with the substituted oxygen moiety available at sixth carbon of quinoline ring. Other residues such as Pro116, Pro126 and Leu156 displayed alkyl interactions with the sitamaquine. Among these Leu156 exhibit alkyl interactions with the quinoline ring and alkyl chain of the ligand whereas Pro116 and Pro126 exhibit alkyl interactions with the methyl and alkyl chain of the ligand.

Among the remaining derivatives, the compounds 10a, 10d, 11a,11c,12a, 12c, and 12dshowed better binding affinity as compared to standard drug sitamaquine. The docking pose and ligand interactions along with bonding types of various derivatives are given in **(Table 4)**.

S. No	Compd No.	Binding Surface	Ligand Interactions	Bonding
1.	10a	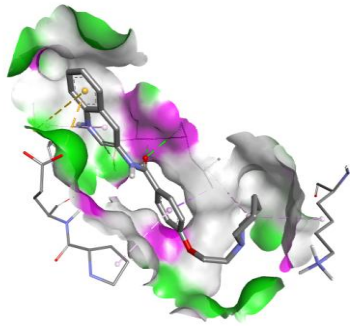	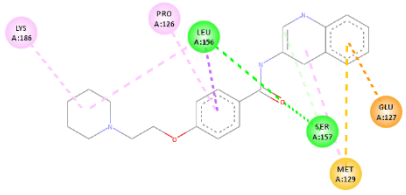	Conventional hydrogen bonding, Carbon hydrogen bond, Pi-anion, pi-sigma, pi-alkyl and pi-sulphur interactions.
2.	10b	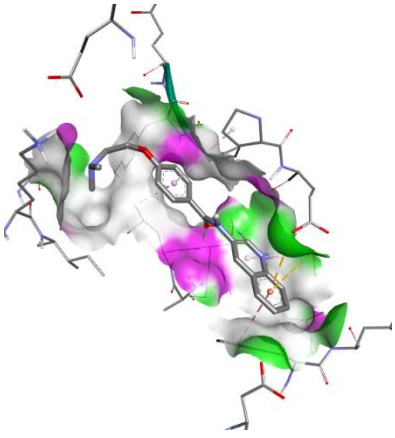	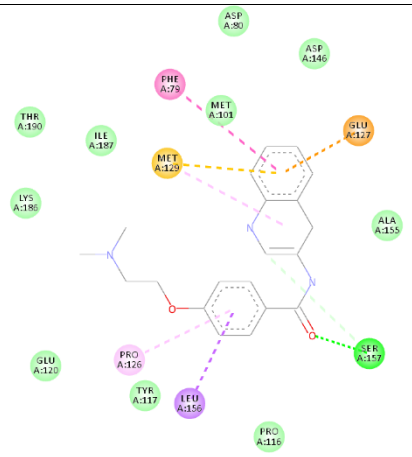	Vander waal bonding, Conventional hydrogen bonding, Carbon hydrogen bond, Pi-anion, pi-sigma, pi-alkyl and pi-sulphur interactions.

Annals of R.S.C.B., ISSN:1583-6258, Vol. 25, Issue 6, 2021, Pages. 10552 - 10570
Received 25 April 2021; Accepted 08 May 2021.

3.	**10c**	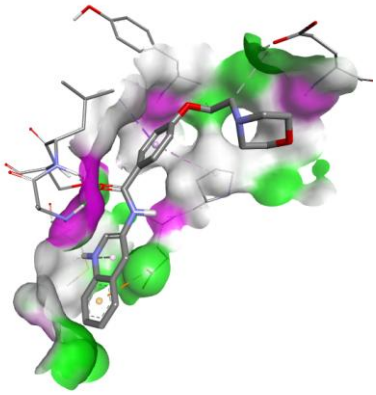	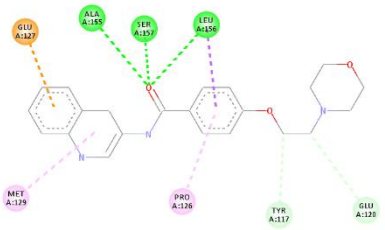	Vander waal bonding, Conventional hydrogen bonding, Carbon hydrogen bond, Pi-anion, pi-sigma, pi-alkyl interactions
4.	**10d**	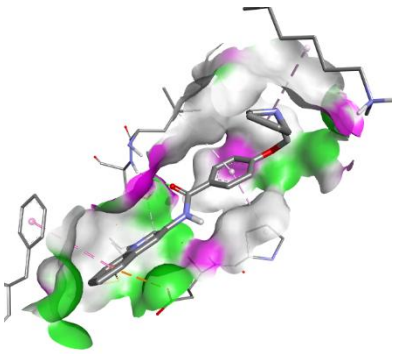	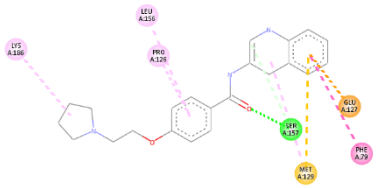	Conventional hydrogen bonding, Carbon hydrogen bond, pi-anion, pi-sulphur, pi-alkyl interactions
5.	**10e**	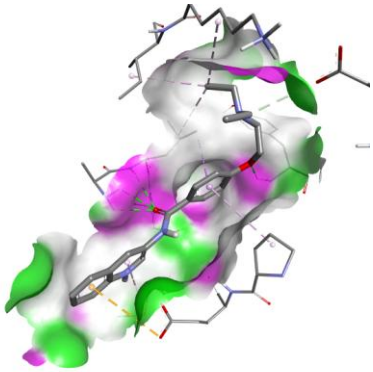	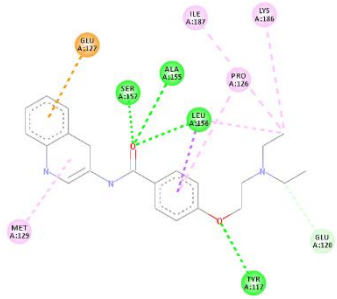	Conventional hydrogen bonding, Carbon hydrogen bond, Pi-anion, pi-sigma, alkyl and pi-alkyl interactions

Annals of R.S.C.B., ISSN:1583-6258, Vol. 25, Issue 6, 2021, Pages. 10552 - 10570
Received 25 April 2021; Accepted 08 May 2021.

6.	**10f**	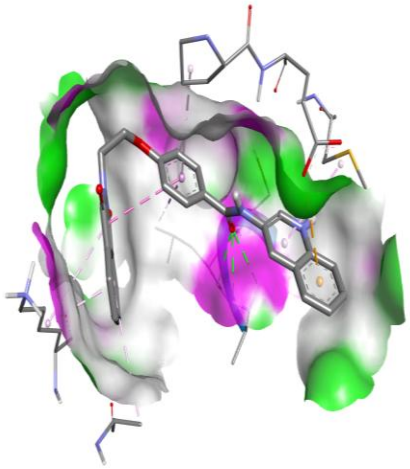	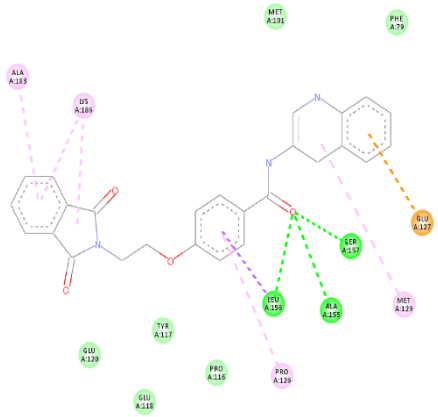	Vander waal, Conventional hydrogen bonding, pi-anion, pi-sigma, alkyl and pi-alkyl interactions.
7.	**11a**	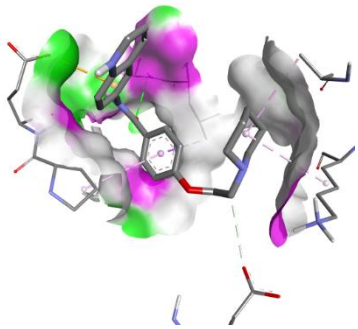	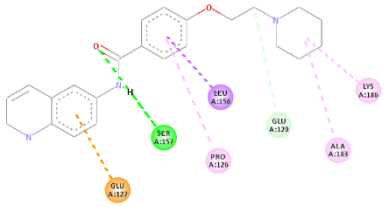	Conventional hydrogen bonding, Carbon hydrogen bond, Pi-anion, pi-sigma, alkyl and pi-alkyl interactions
8.	**11b**	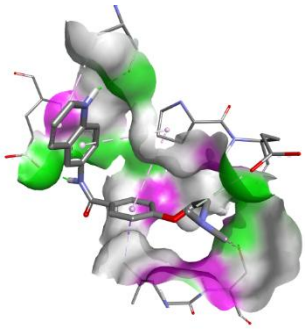	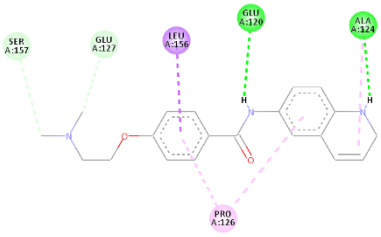	Conventional hydrogen bonding, Carbon hydrogen bond, pi-sigma, alkyl and pi-alkyl interactions

Annals of R.S.C.B., ISSN:1583-6258, Vol. 25, Issue 6, 2021, Pages. 10552 - 10570
Received 25 April 2021; Accepted 08 May 2021.

9.	**11c**	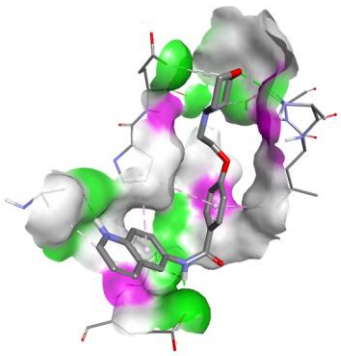	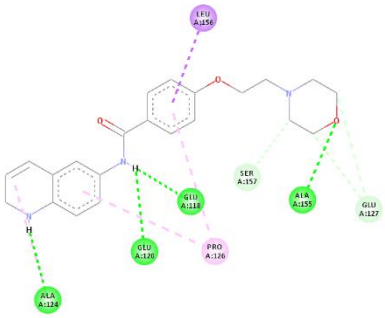	Conventional hydrogen bonding, Carbon hydrogen bond, pi-sigma, alkyl and pi-alkyl interactions
10.	**11d**	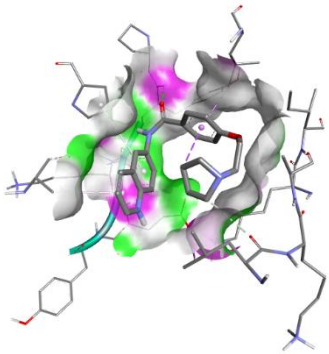	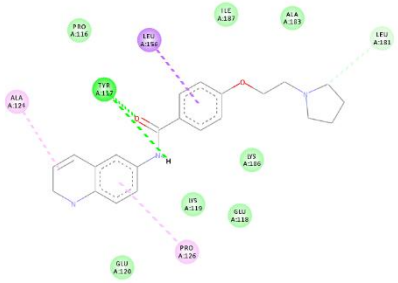	Vander waal, conventional hydrogen bonding, Carbon hydrogen bond, pi-sigma, alkyl and pi-alkyl interactions
11.	**11e**	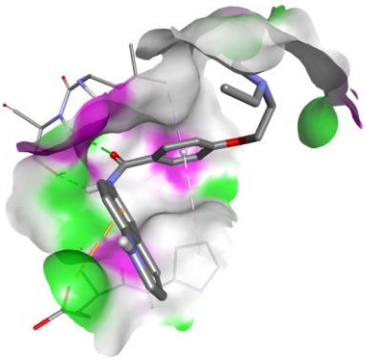	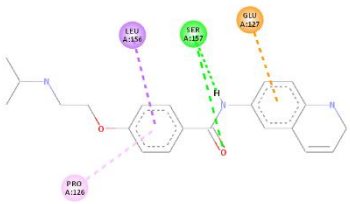	Conventional hydrogen bonding, pi-anion, pi-sigma, and pi-alkyl interactions

Annals of R.S.C.B., ISSN:1583-6258, Vol. 25, Issue 6, 2021, Pages. 10552 - 10570
Received 25 April 2021; Accepted 08 May 2021.

12.	**11f**	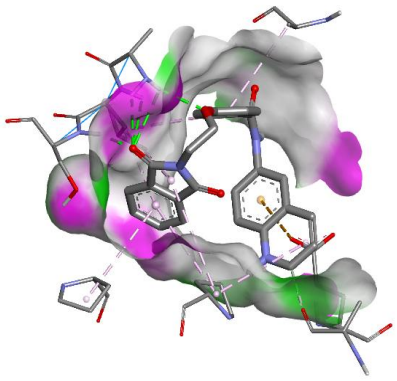	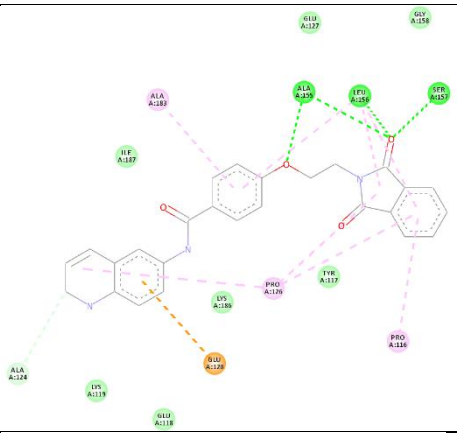	Conventional hydrogen bonding, carbon hydrogen bond, pi-anion, alkyl and pi-alkyl interactions.
13.	**12a**	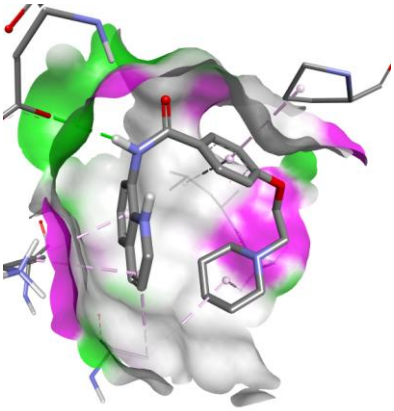	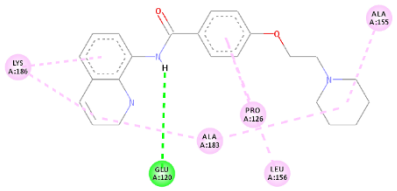	Conventional hydrogen bonding, alkyl and pi-alkyl interactions.
14.	**12b**	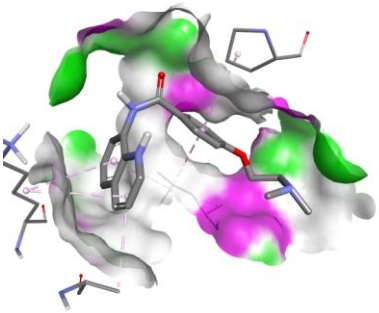	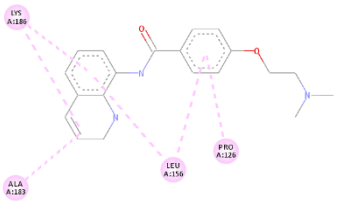	Vander waal, alkyl and pi-alkyl interactions.
15.	**12c**	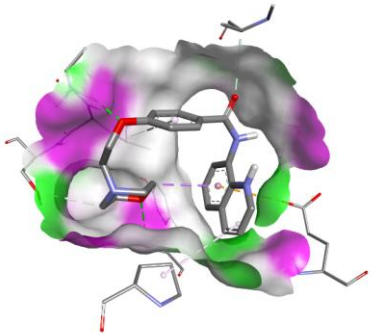	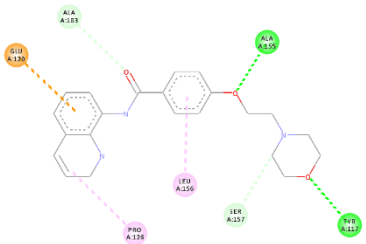	Conventional hydrogen bonding, carbon hydrogen bond, pi-anion, alkyl and pi-alkyl interactions.

Annals of R.S.C.B., ISSN:1583-6258, Vol. 25, Issue 6, 2021, Pages. 10552 - 10570
Received 25 April 2021; Accepted 08 May 2021.

16.	**12d**	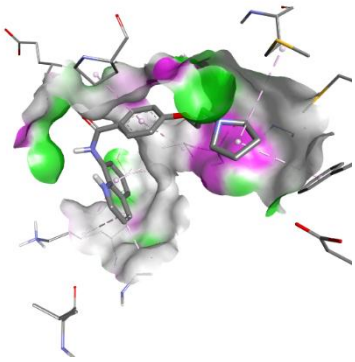	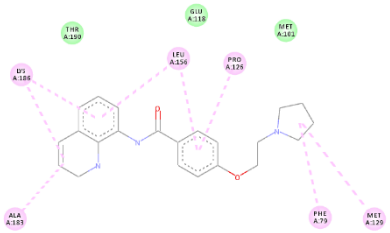	Vander waals, alkyl and pi-alkyl interactions.
17	**12e**	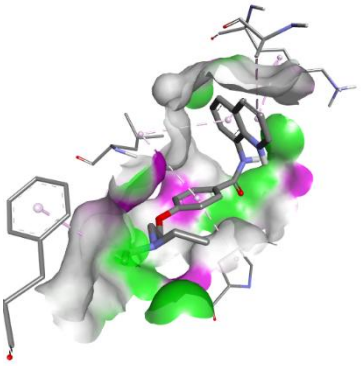	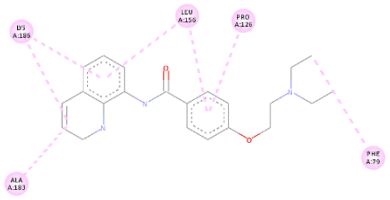	Alkyl and pi-alkyl interactions.
18.	**12f**	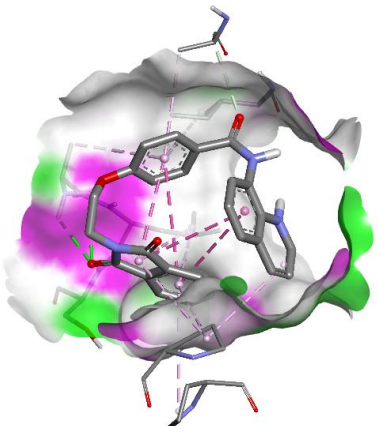	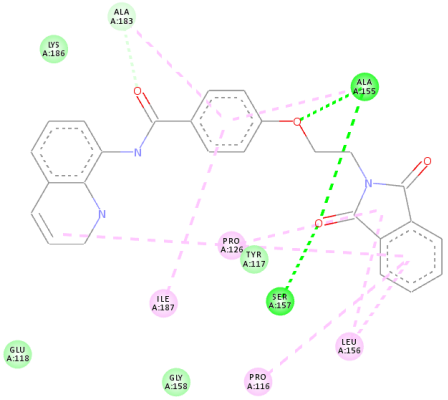	Vander waals, conventional hydrogen bonding, carbon hydrogen bond, alkyl and pi-alkyl interactions.
19.	**Sitamaquine**	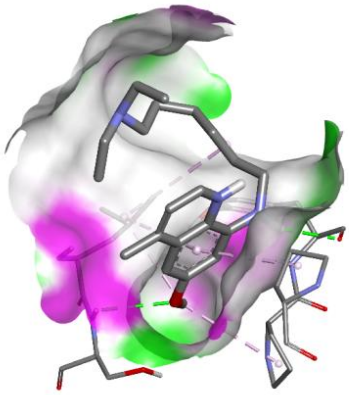	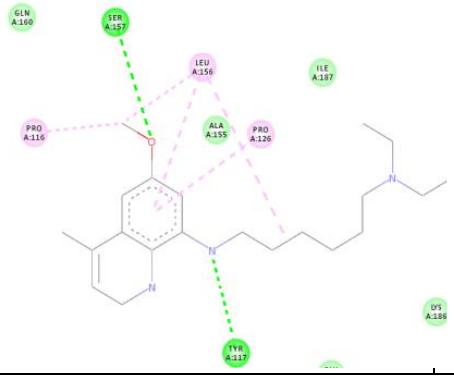	Conventional hydrogen bonding, vander waal, alkyl and pi-alkyl interactions.

Table 4: Binding surface and ligand receptor interaction of various compounds

Annals of R.S.C.B., ISSN:1583-6258, Vol. 25, Issue 6, 2021, Pages. 10552 - 10570
Received 25 April 2021; Accepted 08 May 2021.

Drug-Likeness and ADMET analysis

Drug-likeness assessment and admet investigation for various compounds along with reference drug are given in **(Tables 5)** and **(Table 6)** respectively.

Compound No.	Mass	Log P	PSA	Hydrogen acceptor	Hydrogen donor	Molar refractivity	No. of rotatable bonds
10a	375.19	1.839	53.93	5	1	113.79	7
10b	335.16	0.975	53.93	5	1	107.02	7
10c	377.17	0.649	63.16	6	1	116.1	7
10d	361.18	1.481	53.93	5	1	110.88	7
10e	363.19	1.821	53.93	5	1	115.61	9
10f	437.14	1.098	88.07	7	1	133.63	7
11a	375.19	1.222	53.93	5	1	113.79	7
11b	335.16	0.358	53.93	5	1	107.02	7
11c	377.17	-0.042	63.16	6	1	116.1	7
11d	361.18	0.864	53.93	5	1	110.88	7
11e	363.19	1.204	53.93	5	1	115.61	9
11f	437.14	0.481	88.07	7	1	133.63	7
12a	375.19	1.222	53.93	5	1	113.86	7
12b	335.16	0.358	53.93	5	1	107.1	7
12c	377.17	-0.042	63.16	6	1	116.17	7
12d	361.18	0.864	53.93	5	1	110.95	7
12e	363.19	1.204	53.93	5	1	115.61	9
12f	437.14	0.481	88.07	7	1	133.63	7
Sitamaquine	343.26	3.242	24.50	4	1	94.38	11

Table (5):-Drug-likeness assessment

The outcome of DruLiTo software demonstrate that all the synthesized compounds have admissible physico-chemical properties such as hydrogen-bonding capacity i.e., the numbers of hydrogen bond acceptors are under 10, and hydrogen bond donors are under 5, an important determinant of permeability. The molecular weight of the synthesized compounds is under 500, which predict that these compounds can be easily transported, diffused and absorbed as compared to large molecule. LogP value i.e., the octanol–water partition coefficient that usually quantified molecular lipophilicity is in the range of -0.042-1.839 i.e., under 5 which suggests the good permeability across the cell membrane and the polar surface area (TPSA), which indicates the good bioavailability of the drug molecule is in the range of 53.93-88.07 and is well below the limits. All the values are in acceptable range hence all the synthesized drug molecules follow Lipinski rule of five.

S.no	Compound No.	LogS	Human Intestinal absorption	Caco2 Permeability	Blood-Brain Barrier	T 1/2 (Half Life Time)	LD_{50} mol/kg
1.	**10a**	-5.393	+	-4.997	+++	1.583	2.585
2.	**10b**	-4.747	+	-4.890	+++	1.538	2.495

Annals of R.S.C.B., ISSN:1583-6258, Vol. 25, Issue 6, 2021, Pages. 10552 - 10570
Received 25 April 2021; Accepted 08 May 2021.

3.	**10c**	-4.418	+	-4.984	+++	1.637	2.582
4.	**10d**	-4.986	+	-5.036	+++	1.587	2.605
5.	**10e**	-5.359	+	-4.922	+++	1.708	2.556
6.	**10f**	-5.223	+	-5.163	+++	1.781	2.531
7.	**11a**	-5.421	+	-4.998	+++	1.609	2.582
8.	**11b**	-4.788	+	-4.894	+++	1.635	2.499
9.	**11c**	-4.469	+	-4.985	+++	1.647	2.563
10.	**11d**	-5.008	+	-5.044	+++	1.629	2.602
11.	**11e**	-5.364	+	-4.917	+++	1.705	2.559
12.	**11f**	-5.256	+	-5.167	+++	1.744	2.529
13.	**12a**	-5.365	+	-4.994	+++	1.582	2.585
14.	**12b**	-4.653	+	-4.895	+++	1.552	2.493
15.	**12c**	-4.410	+	-4.980	+++	1.628	2.573
16.	**12d**	-4.966	+	-5.033	+++	1.587	2.618
17.	**12e**	-5.326	+	-4.912	++	1.688	2.550
18	**12f**	-5.217	+	-5.154	++	1.744	2.515
19.	**Sitamaquine**	-5.124	++	-4.664	++	2.213	2.538

Table (6):-ADMET analysis

All the synthesized compounds showed optimal Caco-2 permeability in a range of -4.890 to –5.167. As most of the drugs are administered through the oral route, so it is required that the drug should be highly absorbed in intestinal tissue since all the compounds are HIA positive so they can be easily absorbed by human intestine and also all of them exhibit blood brain-barrier crossing ability. The half-life (T1/2) values of various derivatives were in the range of 1.583 to 1.781 hours. Median lethal dose (LD_{50}) usually represents the acute toxicity of compounds. It is the dose amount of a tested molecule to kill 50 % of the treated animals within a given period. In the present work the LD_{50} of various derivatives is in the comparable range with the reference. Since most of the synthesized compounds showed an acceptable range of ADMET profiles so they can be used efficiently as potent drug candidates.

CONCLUSION

In tropical countries,leishmaniasis is one of the major public issue which is contributing to the mortality and spreading across the globe. The possible therapeutic treatment for leishmaniasis is limited and declined as a result of the rise of widespread resistance and toxicity. Therefore, there is an urgent need of some novel molecules with antileishmanial activity for the treatment of leishmaniasis. The current investigation reports the synthesis, spectral characterization and antileishmanial activity of the newly synthesized series of quinoline derivatives i.e., 10a to 13f. The results of antileishmanial activity revealed that 10a, 10f, 11f, 12a, 12c, 12d and 12f, showed better binding affinity whereas 10c, 10d, 11a and 11c were comparable in their action to standard drug showing good human absorption and better log P values.It can be concluded that these compounds possess significant leishmanicidal property which can lead to generation of lead molecule for the management of leishmaniasis. However, further thorough investigation is desired to appraise their potential of evolving into the therapeutic agents.

ACKNOWLEDGMENTS

Authors are thankful to the Vice-chancellor, Banasthali Vidyapith for providing necessary research facilities. The corresponding author is also thankful to Amity University, Haryana.

Annals of R.S.C.B., ISSN:1583-6258, Vol. 25, Issue 6, 2021, Pages. 10552 - 10570
Received 25 April 2021; Accepted 08 May 2021.

REFERENCES

1. Pink, R., Hudson, A., Mouriès, M. A., & Bendig, M. (2005). Opportunities and challenges in antiparasitic drug discovery. Nature reviews Drug discovery, 4(9), 727-740.. https://doi.org/10.1038/nrd1824
2. World Health Organization. The world health report 2002: reducing risks, promoting healthy life. World Health Organization; 2002.
3. Das, B. B., Ganguly, A., & Majumder, H. K. (2008). DNA topoisomerases of Leishmania: the potential targets for anti-leishmanial therapy. Drug targets in Kinetoplastid parasites, 103-115.doi: 10.1007/978-0-387-77570-8_9
4. Mukhopadhyay, D., Dalton, J. E., Kaye, P. M., & Chatterjee, M. (2014). Post kala-azar dermal leishmaniasis: an unresolved mystery. Trends in parasitology, 30(2), 65-74. https://doi.org/10.1016/j.pt.2013.12.004
5. Berhe, N., Wolday, D., Hailu, A., Abraham, Y., Ali, A., Gebre-Michael, T., ... & Britton, S. (1999). HIV viral load and response to antileishmanial chemotherapy in co-infected patients. Aids, 13(14), 1921-1925. doi: 10.1097/00002030-199910010-00015
6. Roberts, L. J., Handman, E., & Foote, S. J. (2000). Science, medicine, and the future: Leishmaniasis. Bmj, 321(7264), 801-804.https://doi.org/10.1136/bmj.321.7264.801
7. Alvar, J., Vélez, I. D., Bern, C., Herrero, M., Desjeux, P., Cano& WHO Leishmaniasis Control Team. (2012). Leishmaniasis worldwide and global estimates of its incidence. PloS one, 7(5), e35671.https://doi.org/10.1371/journal.pone.0035671
8. Pratt, D. M., & David, J. R. (1981). Monoclonal antibodies that distinguish between New World species of Leishmania. Nature, 291(5816), 581-583.. https://doi.org/10.1038/291581a0
9. Bray, R. S. (1974). Leishmania. Annual Reviews in Microbiology, 28(1), 189-217.
10. Ryan, L., Vexenat, A., Marsden, P. D., Lainson, R., & Shaw, J. J. (1990). The importance of rapid diagnosis of new cases of cutaneous leishmaniasis in pin-pointing the sandfly vector.;84(6):786. doi: 10.1016/0035-9203(90)90080-x.
11. Marsden, P. D., & Lumsden, W. H. (1971). Trypanosomiasis and leishmaniasis. The Practitioner, 207(238), 181-185. PMID: 4998413.
12. Handman, E., & Curtis, J. M. (1982). Leishmania tropica: surface antigens of intracellular and flagellate forms. Experimental parasitology, 54(2), 243-249.https://doi.org/10.1016/0014-4894(82)90133-3
13. Handman, E., Jarvis, H. M., & Mitchell, G. F. (1984). Leishmania major: identification of stage-specific antigens and antigens shared by promastigotes and amastigotes. Parasite immunology, 6(3), 223-233.. https://doi.org/10.1111/j.1365-3024.1984.tb00795.x
14. Lepay, D. A., Nogueira, N., & Cohn, Z. (1983). Surface antigens of Leishmania donovani promastigotes. The Journal of experimental medicine, 157(5), 1562-1572.https://doi.org/10.1084/jem.157.5.1562
15. Chang, K. P., & Fong, D. U. N. N. E. (1982). Antigenic changes during intracellular differentiation of Leishmania mexicana in cultured macrophages. Infection and immunity, 36(1), 430.. DOI: 10.1128/IAI.36.1.430-431.1982
16. Depledge, D. P., MacLean, L. M., Hodgkinson, M. R., Smith, B. A., Jackson, A. P., Ma, S., ... & Smith, D. F. (2010). Leishmania-specific surface antigens show sub-genus sequence variation and immune recognition. PLoS Negl Trop Dis, 4(9), e829.
17. FFraga, J., Montalvo, A. M., De Doncker, S., Dujardin, J. C., & Van der Auwera, G. (2010). Phylogeny of Leishmania species based on the heat-shock protein 70 gene. Infection, Genetics and Evolution, 10(2), 238-245.https://doi.org/10.1016/j.meegid.2009.11.007
18. Sacks, D. L. (2001). Leishmania–sand fly interactions controlling species-specific vector competence: Microreview. Cellular microbiology, 3(4), 189-196.https://doi.org/10.1046/j.1462-5822.2001.00115.x
19. Murray, H. W., Pépin, J., Nutman, T. B., Hoffman, S. L., & Mahmoud, A. A. (2000). Tropical medicine. Bmj, 320(7233), 490-494.
20. Pérez-Victoria, F. J., Sánchez-Cañete, M. P., Seifert, K., Croft, S. L., Sundar, S., Castanys, S., & Gamarro, F. (2006). Mechanisms of experimental resistance of Leishmania to miltefosine: implications for clinical use. Drug Resistance Updates, 9(1-2), 26-39.https://doi.org/10.1016/j.drup.2006.04.001
21. Joule, J. A., & Mills, K. (2012). Heterocyclic chemistry at a glance. John Wiley & Sons.

22. Pozharskii, A. F., Soldatenkov, A. T., & Katritzky, A. R. (2011). Heterocycles in life and society: an introduction to heterocyclic chemistry, biochemistry and applications. John Wiley & Sons.
23. Katritzky, A. R., Ramsden, C. A., Joule, J. A., & Zhdankin, V. V. (2010). Handbook of heterocyclic chemistry. Elsevier.
24. Eicher, T., Hauptmann, S., & Speicher, A. (2013). The chemistry of heterocycles: Structures, reactions, synthesis, and applications. John Wiley & Sons.
25. Abas, F., Lajis, N. H., Israf, D. A., Khozirah, S., & Kalsom, Y. U. (2006). Antioxidant and nitric oxide inhibition activities of selected Malay traditional vegetables. Food Chemistry, 95(4), 566-573.https://doi.org/10.1016/j.foodchem.2005.01.034
26. Chen, Y. L., Chen, I. L., Tzeng, C. C., & Wang, T. C. (2000). Synthesis and Cytotoxicity Evaluation of Certain α-Methylidene-γ-butyrolactones Bearing Coumarin, Flavone, Xanthone, Carbazole, and Dibenzofuran Moieties. Helvetica Chimica Acta, 83(5), 989-994.. https://doi.org/10.1002/(SICI)1522-2675(20000510)83:5
27. Atwell, G. J., Baguley, B. C., & Denny, W. A. (1988). Potential antitumor agents. 55. 6-Phenylphenanthridine-4-carboxamides: a new class of DNA-intercalating antitumor agents. Journal of medicinal chemistry, 31(4), 774-779.https://doi.org/10.1021/jm00400a029
28. Ashutosh, S. G., & Ramesh, S. S. (2005). Use of Leishmania donovani field isolates expressing the luciferase reporter gene in in vitro drug screening. Antimicrobial agents and chemotherapy, 49(9), 3776.. doi: 10.1128/AAC.49.9.3776-3783.2005
29. Biovia, D. S., & Dsme, R. (2019). San Diego: Dassault Systèmes.
30. Eisenberg, D., Lüthy, R., & Bowie, J. U. (1997). [20] VERIFY3D: assessment of protein models with three-dimensional profiles. Methods in enzymology, 277, 396-404.https://doi.org/10.1016/S0076-6879(97)77022-8
31. Lüthy, R., Bowie, J. U., & Eisenberg, D. (1992). Assessment of protein models with three-dimensional profiles. Nature, 356(6364), 83-85. https://doi.org/100.1038/356083a0
32. Trott, O., & Olson, A. J. (2010). AutoDock Vina: improving the speed and accuracy of docking with a new scoring function, efficient optimization, and multithreading. Journal of computational chemistry, 31(2), 455-461.https://doi.org/10.1002/jcc.21334
33. Yamashita, F., & Hashida, M. (2004). In silico approaches for predicting ADME properties of drugs. Drug metabolism and pharmacokinetics, 19(5), 327-338.. https://doi.org/10.2133/dmpk.19.327
34. Mälkiä, A., Murtomäki, L., Urtti, A., & Kontturi, K. (2004). Drug permeation in biomembranes: in vitro and in silico prediction and influence of physicochemical properties. European Journal of Pharmaceutical Sciences, 23(1), 13-47.https://doi.org/10.1016/j.ejps.2004.05.009
35. Van De Waterbeemd, H., & Gifford, E. (2003). ADMET in silico modelling: towards prediction paradise?. Nature reviews Drug discovery, 2(3), 192-204.. https://doi.org/10.1038/nrd1032
36. Bickerton, G. R., Paolini, G. V., Besnard, J., Muresan, S., & Hopkins, A. L. (2012). Quantifying the chemical beauty of drugs. Nature chemistry, 4(2), 90-98.. https://doi.org/10.1038/nchem.1243
37. http://www.niper.gov.in/pi_dev_tools/ DruLiToWeb/DruLiTo_index.html.
38. Lipinski, C. A., Lombardo, F., Dominy, B. W., & Feeney, P. J. (1997). Experimental and computational approaches to estimate solubility and permeability in drug discovery and development settings. Advanced drug delivery reviews, 23(1-3), 3-25.. https://doi.org/10.1016/S0169-409X(96)00423-1
39. Dong, J., Wang, N. N., Yao, Z. J., Zhang, L., Cheng, Y., Ouyang, D., ... & Cao, D. S. (2018). ADMETlab: a platform for systematic ADMET evaluation based on a comprehensively collected ADMET database. Journal of cheminformatics, 10(1), 1-11.. https://doi.org/10.1186/s13321-018-0283-x